Supplementary Information for "On the origins of temporal power-law behavior in the global atmospheric circulation"

Dmitry I. Vyushin, Paul J. Kushner, Josh Mayer

Department of Physics, University of Toronto, Toronto, Ontario, Canada

DFA3 vs GSPE

Several H estimation methods are available (*Vyushin and Kushner*, 2009) and we test here whether some of our key results are method dependent. In the original Figs. 1 and 2 we used the DFA3 time domain H estimator. *Vyushin and Kushner* (2009) have shown that DFA3 and other spectral domain methods yield consistent estimates of H provided a consistent frequency range has been chosen and known climate signals have been filtered out. DFA3 effectively filters out linear and quadratic trends in the data, which helps us to focus on internal climate variability. The distribution of the DFA3 $\hat{H}$ seems to be Gaussian (*Rybski and Bunde*, 2009) with standard deviation ≈ 0.075 for the case of the time scale range of 18 to 540 time units (*Vyushin and Kushner*, 2009; *Weron*, 2002). Overall, DFA3 provides more robust estimates than other available methods, but for the results reported here, we have found consistent results using the spectral domain Gaussian semiparametric estimator.

Supplementary Figs. 1 and 2 apply Gaussian Semiparametric Estimator (GSPE, *Robinson*, 1995) to the same data sets as in the original Figs. 1 and 2. GSPE is a maximum-likelihood spectral domain estimator of H. The GSPE $\hat{H}$ is known to be relatively sensitive to the presence of linear and nonlinear trends and to high-frequency spectral peaks compared to DFA3 (*Vyushin and Kushner*, 2009). Because of the known sensitivity to trends we have filtered out linear trend before calculating the GSPE $\hat{H}$.

In supplementary Fig. 1 the overall distribution of the GSPE $\hat{H}$ is similar to, but noisier than, the DFA3 $\hat{H}$ in the original Fig. 1. However, significant differences remain. For example, Southern Hemisphere stratospheric values of $\hat{H}$ are larger for GSPE than for DFA3

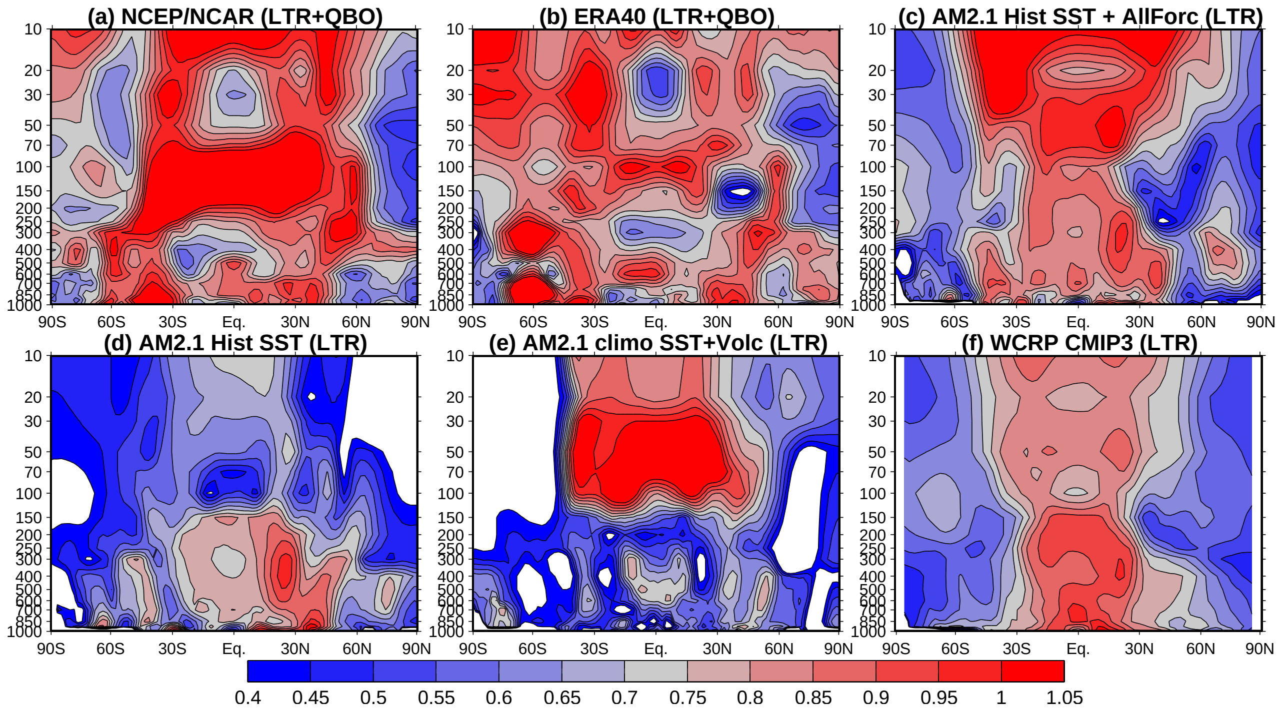

Figure 1: $\hat{H}$ distribution estimated by GSPE for zonal-mean temperature for (a) the NCEP/NCAR reanalysis, (b) the ERA40 reanalysis, (c) the GFDL AM2.1 HistSST+AllForc simulation, (d) the GFDL AM2.1 HistSST simulation, (e) the GFDL AM2.1 Vol simulation, (f) the CMIP3 simulations. Panel (f) represents a multiple model average. As stated in the text, QBO filtering has been applied to the reanalysis temperatures in Figs. 1a-b. Values of $\hat{H}$ less than 0.4 are shown in white.

in the reanalyses due to nonlinear trends from ozone depletion and data inhomogeneities. In addition, the differences in the tropical troposphere arise from ENSO related variability that boosts the high frequencies and is known to reduce the GSPE $\hat{H}$ relative to the DFA3 $\hat{H}$ (*Vyushin and Kushner*, 2009). In the CMIP3 simulations this discrepancy is present when we analyze 45 year long time series, but is reduced when we analyze 100 year long time series.

We also have to bear in mind GSPE's sensitivity to high frequency spectral peaks when we try to reproduce the results of Fig. 2, which illustrates the sensitivity of $\hat{H}$ to tropical SST variability. The impact on the GSPE $\hat{H}$ of TropSST (*Smith et al.*, 2008) filtering (not shown)

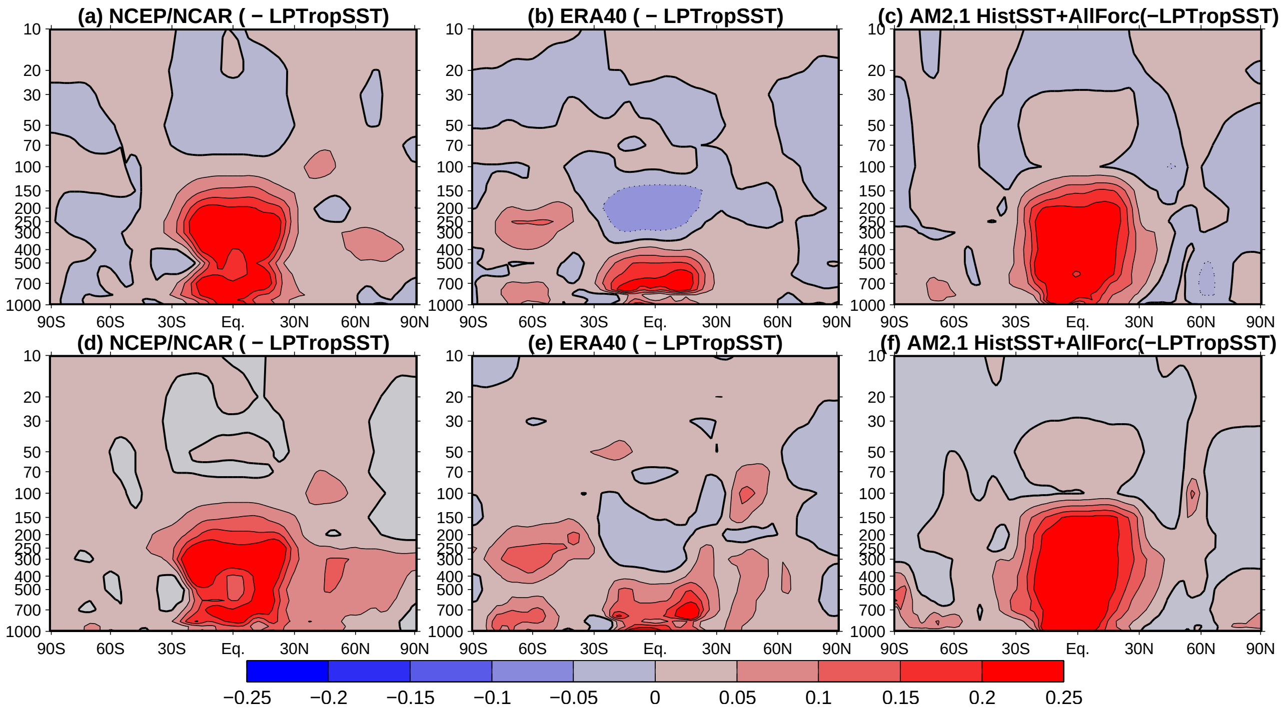

Figure 2: $\hat{H}$ without LPTropSST filtering minus $\hat{H}$ with LPTropSST filtering, which represents the signature of the tropical SSTs in the $\hat{H}$ field. First row - DFA3 estimates, second row - GSPE estimates.

looks quite different from that for the DFA3 $\hat{H}$, which is shown in the original Figs. 2d-f. This difference arises because the high frequency component of the TropSST signal dominates the GSPE $\hat{H}$ response while the low frequency component of the TropSST signal dominates the DFA3 $\hat{H}$ response. But we can put the two methods on a more even footing by focusing on the decadal component of the Tropical SST variability, which is the timescale of interest in this study. To do so, we construct a 3 year low-pass filtered tropically averaged SST signal ("LPTropSST") and compute the response to LPTropSST filtering in DFA3 $\hat{H}$and GSPE $\hat{H}$ in supplementary Fig. 2. The first raw of this figure is similar to the original Fig. 2, showing that the DFA3 $\hat{H}$ response is robust to the low-pass filtering. The first and the second raw of the supplementary Fig. 2 are also remarkably similar, indicating that the tropical SST effect is in good agreement in the two methods.

An open source R package that includes various spectrum and the Hurst exponent estimators as well as both AR1-based and power-law-based trend detection algorithms is available.

Effect of volcanic eruptions

We return to the volcanic signature of $\hat{H}$ in the lower stratosphere. It has been shown theoretically that a sum of stochastic amplitude shocks decaying by a power law has a power law spectrum (*Parke*, 1999). But the volcanically induced warming of the stratosphere decays exponentially in time (*Robock*, 2000) and so we cannot expect power-law behavior in temperature except over a limited range of frequencies.

A simple model to capture the behavior is

$$\frac{dT}{dt} = -\frac{1}{\tau}T + V(t) \tag{1}$$

where T is temperature, τ is a relaxation time scale and $V(t)$ is the volcanic forcing (*Stenchikov et al.*, 2006) (expressed as aerosol optical depth). Supplementary Fig. 3a shows one-year running mean air temperature anomalies in the tropical lower stratosphere obtained from the GFDL AM2.1 Vol simulation (see the original Fig. 1e), Fig. 3b the solutions to (1) for various values of τ, and Fig. 3c the power spectra for the time series in Fig. 3b. As the relaxation time scale gets larger the power spectra saturate at lower frequencies, which would give rise to larger estimates of H. These power spectra demonstrate a combination of power-law behavior between 6 months and 4-10 years and a flat spectrum at the lowest frequencies. When we repeat the same calculation for the volcanic forcing record of the past 130 years the saturation occurs at lower frequency (not shown).

The DFA3 $\hat{H}$ for the solutions to (1) are labelled with colors corresponding to the spectra in Fig. 3c. The $\hat{H}$ values are so large because our simple model does not include regular weather noise, which boosts spectral power in high-frequencies and thus decreases the $\hat{H}$. To support this we have plotted the power spectrum of the solution to (1) for $\tau = 1$ with the weather noise superimposed on it. We employed the time series of air temperature monthly mean anomalies at the equator at 70hPa obtained from the Climo simulation of GFDL AM2.1 that was forced with climatological SSTs and with time-independent radiative forcings. The

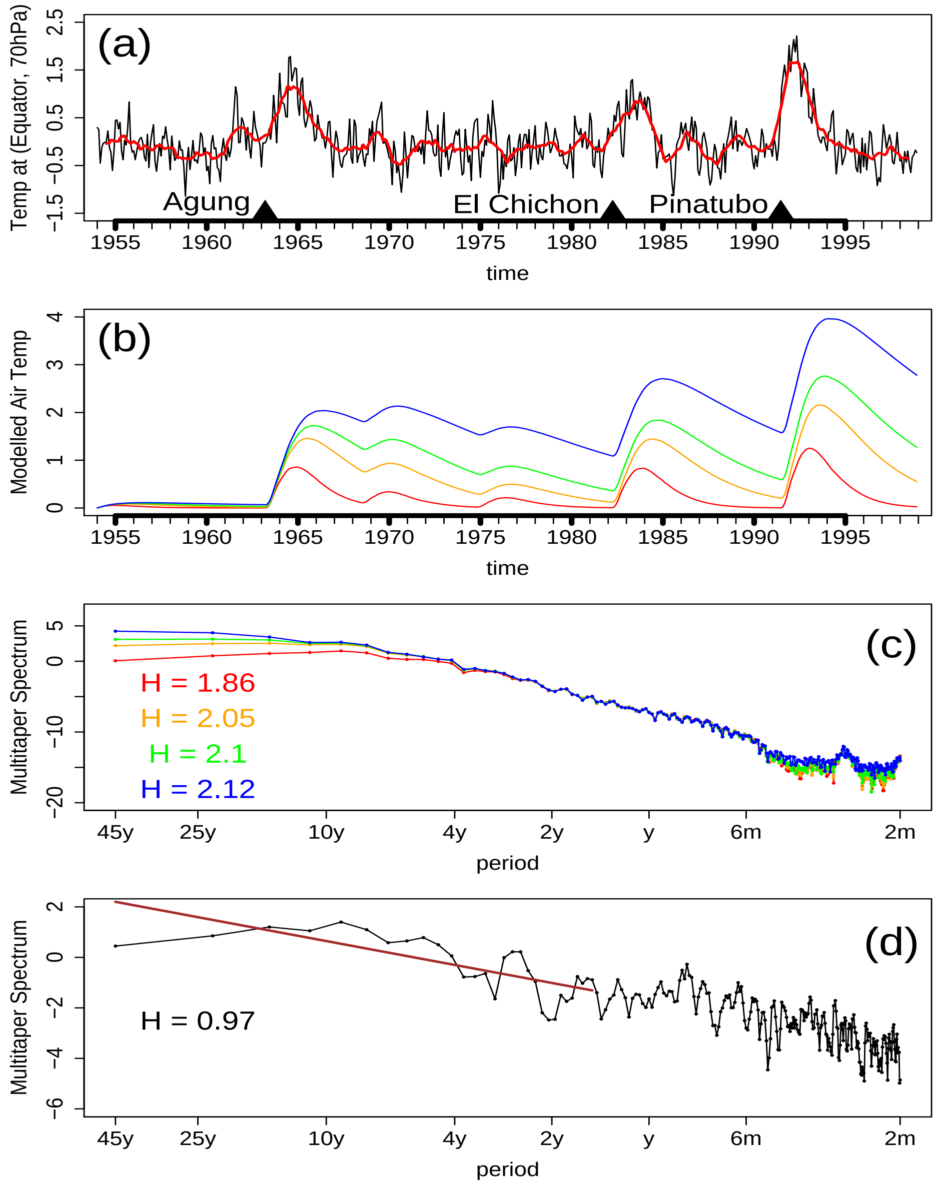

Figure 3: (a) Air temperature anomalies at (Equator, 70hPa) from the AM2.1 Vol simulation. The smooth red curve is a one year running average. The timing and the names of the major volcanic eruptions are shown above the time axis. (b) Solutions to equation (1) for $\tau = 1$ year (red curve), 3 (orange), 5 (green), and 10 years (blue). (c) Multitapered power spectra of these solutions and their DFA3 Hurst exponent estimates. (d) The power spectrum of the solution for $\tau = 1$ with the weather noise superimposed on it. The best fit power-law curve (line in log-log coordinates) is shown in brown. Panels (c-d) are plotted in log-log coordinates.

Hurst exponent estimate of this time series, obtained using the DFA3 method, is 0.97, which agrees well with the values in the lower tropical stratosphere in the original Fig. 1e.

List of possible origins of power-law spectral behavior

We provide a list of some proposed physical processes that generate power-law spectral ($1/f$ noise) behavior and that might be relevant to interannual to decadal scale climate variability: aggregation of multiple scales (*Granger*, 1980; *Caballero et al.*, 2002), in particular in self-organized criticality type models (*Rios and Zhang*, 1999; *Maslov et al.*, 1999); stochastically forced diffusion equation (*Pelletier*, 2002; *Fraedrich et al.*, 2004); nonlinear stochastic differential equations (*Naidenov and Kozhevnikova*, 2000; *Kaulakys et al.*, 2006); a sum of slowly decaying intermittent shocks (*Cox*, 1984; *Parke*, 1999; *Mandelbrot*, 2003); point processes (*Davidsen and Schuster*, 2002; *Kaulakys et al.*, 2005); chaotic Hamiltonian dynamics (*Geisel et al.*, 1987; *Zaslavsky*, 2002); intermittent nonlinear maps (*Barenco and Arrowsmith*, 2004; *Miyaguchi and Aizawa*, 2007), etc.

GCMs details

The 17 CMIP3 models used in our study are CGCM3.1(T47), CGCM3.1(T63), CSIRO-Mk3.0, CSIRO-Mk3.5, ECHAM5/MPI-OM, GFDL-CM2.0, GFDL-CM2.1, GISS-AOM, GISS-EH, GISS-ER, MIROC3.2(medres), MIROC3.2(hires), MRI-CGCM2.3.2, NCAR CCSM3.0, NCAR PCM, UKMO-HadCM3, UKMO-HadGEM1. We have chosen the most established models among all available CMIP3 models. We used one 20C3M run from each model. The details of the models have been documented previously (*Santer et al.*, 2005; *Stenchikov et al.*, 2006) and can also be found on the CMIP3 web-site.

References

Barenco, M., and D. K. Arrowsmith (2004), The autocorrelation of double intermittency maps and the simulation of computer packet traffic, *Dynamical Systems*, *19*, 61–74.

Caballero, R., S. Jewson, and A. Brix (2002), Long memory in surface air temperature: detection, modeling, and application to weather derivative valuation, *Climate Research*, *21*, 127–140.

Cox, D. R. (1984), Long-Range Dependence: A Review, in *Statistics: An Appraisal. Proceedings 50th Anniversary Conference Iowa State Statistical Laboratory*, edited by H. A. David and H. T. David, pp. 55–74, The Iowa State University Press.

Davidsen, J., and H. G. Schuster (2002), Simple model for $1/f^{\alpha}$ noise, *Phys. Rev. E*, *65*, 026,120, doi:10.1103/PhysRevE.65.026120.

Fraedrich, K., U. Luksch, and R. Blender (2004), 1/f-model for long-time memory of the ocean surface temperature, *Phys. Rev. E*, *70*, 037,301(1–4).

Geisel, T., A. Zacherl, and G. Radons (1987), Generic 1/f noise in chaotic Hamiltonian dynamics, *Phys. Rev. Lett.*, *59*, 2503–2506.

Granger, C. W. J. (1980), Long memory relationships and the aggregation of dynamic models, *J. Econometrics*, *14*, 227–238.

Kaulakys, B., V. Gontis, and M. Alaburda (2005), Point process model of 1/f noise vs a sum of Lorentzians, *Phys. Rev. E*, *71*, 051,105, doi:10.1103/PhysRevE.71.051105.

Kaulakys, B., J. Ruseckas, V. Gontis, and M. Alaburda (2006), Nonlinear stochastic models of 1/f noise and power-law distributions, *Physica A*, *365*, 217–221, doi:10.1016/j.physa.2006.01.017.

Mandelbrot, B. B. (2003), Fractal sums of pulses and a practical challenge to the distinction between local and global dependence, in *Processes with Long-Range Correlations*, edited by G. Rangarajan and M. Ding, pp. 118–138, Springer.

Maslov, S., C. Tang, and Y.-C. Zhang (1999), 1/f noise in Bak-Tang-Wiesenfeld models on narrow stripes, *Phys. Rev. Lett.*, *83*, 2449–2452.

Miyaguchi, T., and Y. Aizawa (2007), Spectral analysis and an area-preserving extension of a piecewise linear intermittent map, *Phys. Rev. E*, *75*, 066,201, doi:10.1103/PhysRevE.75.066201.

Naidenov, V. I., and I. A. Kozhevnikova (2000), A hydrophysical mechanism of the Hurst phenomenon, *Doklady Physics*, *45*, 336–338, doi:10.1134/1.1307084.

Parke, W. R. (1999), What is fractional integration?, *The Review of Economics and Statistics*, *81*, 632–638.

Pelletier, J. D. (2002), Natural variability of atmospheric temperatures and geomagnetic intensity over a wide range of time scales, *Proc. Natl. Acad. Sci. (USA)*, *99*, 2546–2553.

Rios, P. D. L., and Y.-C. Zhang (1999), Universal 1/f noise from dissipative self-organized criticality models, *Phys. Rev. Lett.*, *82*, 472–475.

Robinson, P. M. (1995), Gaussian estimation of long range dependence, *Ann. Statist.*, *23*, 1630–1661.

Robock, A. (2000), Volcanic eruptions and climate, *Rev. Geophys.*, *38*, 191–219.

Rybski, D., and A. Bunde (2009), On the detection of trends in long-term correlated records, *Physica A*, *388*, 1687–1695, doi:10.1016/j.physa.2008.12.026.

Santer, B. D., T. M. L. Wigley, C. Mears, F. J. Wentz, and S. A. Klein (2005), Amplification of surface temperature trends and variability in the tropical atmosphere, *Science*, *309*, 1551–1556, doi:10.1126/science.1114867.

Smith, T. M., R. W. Reynolds, T. C. Peterson, and J. Lawrimore (2008), Improvements to NOAA's historical merged land-ocean surface temperature analysis (1880-2006), *J. Climate*, *21*, 2283–2296.

Stenchikov, G., K. Hamilton, R. J. Stouffer, A. Robock, V. Ramaswamy, B. Santer, and H.-F. Graf (2006), Arctic Oscillation response to volcanic eruptions in the IPCC AR4 climate models, *J. Geophys. Res.*, *111*, D07,107.

Vyushin, D. I., and P. J. Kushner (2009), Power-law and long-memory characteristics of the atmospheric general circulation, *J. Climate (in press)*.

Weron, R. (2002), Estimating long-range dependence: finite sample properties and confidence intervals, *Physica A*, *312*, 285–299.

Zaslavsky, G. M. (2002), Chaos, fractional kinetics, and anomalous transport, *Phys. Rep.*, *371*, 461–580.